Journal of Molecular Graphics and Modelling 28 (2010) 807–813

Contents lists available at ScienceDirect

Journal of Molecular Graphics and Modelling

journal homepage: www.elsevier.com/locate/JMGM

Stereoelectronic interaction effects on the conformational properties of hydrogen peroxide and its analogues containing S and Se atoms: An ab initio, hybrid-DFT study and NBO analysis

Davood Nori-Shargh[a,b], Hooriye Yahyaei[b], James E. Boggs[a,*]

[a] Institute for Theoretical Chemistry, Chemistry and Biochemistry Department, The University of Texas at Austin, Austin, TX 78712-0165, United States
[b] Chemistry Department, Science and Research Campus, Islamic Azad University, Tehran, Iran

ARTICLE INFO

Article history:
Received 15 December 2009
Received in revised form 5 February 2010
Accepted 9 February 2010
Available online 18 February 2010

Keywords:
Molecular modeling
Ab initio
NBO
Hydrogen disulfide
Hydrogen diselenide

ABSTRACT

Ab initio molecular orbital (MP2/6-311+G**//MP2/6-31G+G**) and hybrid-density functional theory (B3LYP/6-311+G**//MP2/6-311+G**) methods and NBO analysis were used to study the stereoelectronic interaction effects on the conformational properties of hydrogen peroxide (**1**), hydrogen disulfide (**2**) and hydrogen diselenide (**3**). The results showed that the Gibbs free energy difference ($G_T - G_S$) values at 298.15 K and 1 atm between the skew (*S*) and trans (*T*) conformations (ΔG_{T-S}) increase from compound **1** to compound **2** but decrease from compound **2** to compound **3**. The *C* conformations of compounds **1**–**3** are less stable than their *S* and *T* conformations. Based on these results, the racemization processes of the axial symmetrical (C_2 symmetry) conformations of compounds **1**–**3** take place *via* their *T* conformations. Based on the optimized ground state geometries using the MP2/6-311+G** level of theory, the NBO analysis of donor–acceptor (bond–antibond) interactions revealed that the stabilization (resonance) energy associated with $LP_2M2 \rightarrow \sigma^*_{M3\text{-}H4}$ electronic delocalization for the *S* conformations of compounds **1**–**3** are 1.35, 5.94 and 4.68 kcal mol^{-1}, respectively. There is excellent agreement between the variations of the calculated ΔG_{T-S} and stabilization (resonance) energies associated with $LP_2M2 \rightarrow \sigma^*_{M3\text{-}H4}$ electronic delocalization for the *S* conformations of compounds **1**–**3**. The correlations between resonance energies, orbital integrals, dipole moments, bond orders, structural parameters and conformational behaviors of compounds **1**–**3** have been investigated. Test were made of complete basis set methods (CBS-QB3, CBS-4 and CBS-Q), the first two gave results essentially indistinguishable from those we used, but the CBS-Q results were in disagreement with experimental and other theoretical results.

© 2010 Elsevier Inc. All rights reserved.

1. Introduction

Hydrogen peroxide, H_2O_2 (**1**), is a well known strong oxidizing agent that occurs naturally in the earth's atmosphere [1–7]. H_2O_2 forms complexes with alkali cations by electrostatic interactions and also with halides and organic molecules by forming a hydrogen bond [8].

Hydrogen disulfide, H_2S_2 (**2**), which can be formed by a self-reaction of SH radicals in the atmosphere [9], has been the subject of extensive theoretical and experimental studies [10–24].

Hydrogen diselenide, H_2Se_2 (**3**), has a tendency to undergo structural reorganization into the free element and its simplest dihydrogen compound, therefore, there are no reported experimental data concerning the properties of compound **3** [25]. However, the conformational properties of compound **3** have been investigated theoretically [26].

Although there is a lot of published experimental and theoretical data for compounds **1** [1–8,28–30] and **2** [9–24,31–41] and also a little for compound **3** [26], there is no published experimental or quantitative theoretical data about the donor–acceptor delocalization effects on the conformational properties of compounds **1**–**3**. In this work, the stereoelectronic interaction effects, dipole–dipole interactions and also the conformational and structural properties of compounds **1**–**3** have been investigated computationally using both ab initio MO and DFT methods (see Scheme 1 and Fig. 1) [42–46].

Since the preferred geometry of many molecules can be viewed as the result of the maximization of an interaction between the best donor lone pair or bond and the best acceptor bond, therefore, stereoelectronic interactions are expected to play an important role on the conformational properties of chemical compounds [47].

In this work, the stabilization energies (E_2) associated with $LP_2M2 \rightarrow \sigma^*_{M3\text{-}H4}$ delocalizations (see Fig. 2) and their influences

* Corresponding author.
E-mail address: james.boggs@mail.utexas.edu (J.E. Boggs).

1093-3263/$ – see front matter © 2010 Elsevier Inc. All rights reserved.
doi:10.1016/j.jmgm.2010.02.006

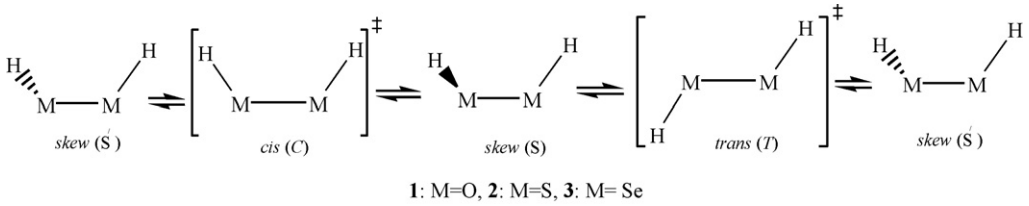

Scheme 1.

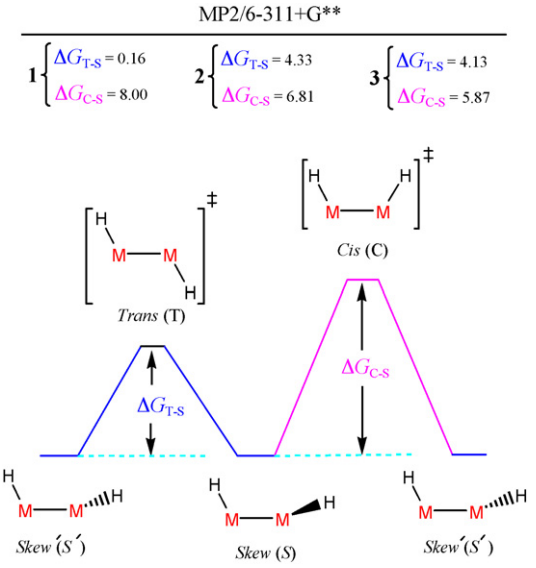

Fig. 1. MP2/6-311+G** calculated energy profiles of the enantiomerization processes for the chiral skew (*S*) conformations of compounds **1**–**3**.

on the conformational properties of compounds **1**–**3** were quantitatively investigated by NBO (natural bond orbital) analysis [48,49]. The resonance energy associated with donor–acceptor electronic delocalization is proportional to $S^2/\Delta E$ where S is the orbital integral of the two interacting orbitals and ΔE is the energy difference between the donor and acceptor orbitals [50]:

$$E_2 \text{ (stabilization or resonance energy) } \alpha \left(\frac{S^2}{\Delta E}\right)$$

In addition, the resonance (stabilization) energy (E_2) associated with $i \rightarrow j$ delocalization, is explicitly estimated by the following equation:

$$E_2 = q_i \frac{F^2(i,j)}{\varepsilon_j - \varepsilon_i}$$

where q_i is the *i*th donor orbital occupancy, ε_i, ε_j are diagonal elements (orbital energies) and $F(i,j)$ off-diagonal elements, respectively associated with the NBO Fock matrix. Therefore, there is a direct relationship between $F(i,j)$ off-diagonal elements and the orbital overlap (S).

2. Computational details

The ab initio molecular orbital and hybrid-DFT calculations were performed using the GAUSSIAN 03 package of programs [42]. Second order Møller–Plesset perturbation theory (MP2) was used with the standard split valence 6-311+G** on all atoms (MO: MP2/6-311+G**). The hybrid-density functional theory (hybrid-DFT: B3LYP/6-311+G**//MP2/6-311+G**) method was used for single-point calculations.

After this work was completed, it was suggested to us that we might obtain higher accuracy by using the complete basis set methods CBS-4, CBS-Q and CBS-QB3 [51–57]. The CBS models are compound methods that extrapolate to the CBS limit by using the N-1 asymptotic convergence of MP2 pair energies calculated from pair natural orbital expansions [51–57]. CBS-4 is a six-step method that starts with UHF/3-21G* geometry and frequency calculations, followed by UHF, CBS2, MP4(SDQ) and empirical corrections [54]. CBS-Q is a seven-step method that starts with MP2(FC)/6-31G† geometry optimization and then UHF/6-31G† frequency calculations, followed by UHF, CBS2, MP4(SDQ), QCISD(T) and empirical corrections [54]. Finally, CBS-QB3 is a modified version of CBS-Q in which the structure optimization and frequency calculations are performed at the B3LYP/CBSB7 level of theory, which gives both improved reliability (maximum error for the G2 test set reduced from 3.9 to 2.8 kcal/mol) and increased accuracy (mean absolute error reduced from 0.98 to 0.87 kcal/mol), with little penalty in computational speed [57].

The NBO analysis was performed at the MP2/6-311+G** level for the skew (*S*) conformations of compounds **1**–**3** by the NBO 3.1 program included in the GAUSSIAN 98 package of programs.

The bonding and antibonding orbital occupancies in the *S* conformations of compounds **1**–**3**, and also the stabilization energies associated with $LP_2M2 \rightarrow \sigma^*_{M3\text{-}H4}$ delocalizations were calculated using NBO analysis. The stabilizing orbital interaction is inversely proportional to the energy difference between the interacting orbitals, therefore the strongest stabilizing interactions will take place between the most effective donors and the most effective acceptors (see Fig. 2).

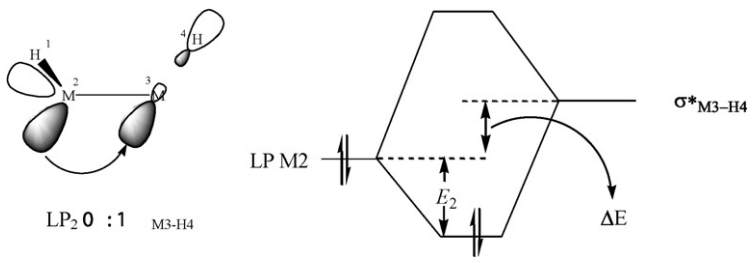

Fig. 2. Schematic representation of the electronic delocalization from LP_2M2 nonbonding and $\sigma^*_{M3\text{-}H4}$ antibonding orbitals and the second order perturbational energy associated with $LP_2M2 \rightarrow \sigma^*_{M3\text{-}H4}$ electronic delocalizations.

Table 1
MP2/6-311+G**//MP2/6-311+G**and B3LYP/6-311+G**//MP2/6-311+G** calculated total energies *E*, zero-point energies *ZPE* (from MP2/6-311+G**level) and relative energies ΔE (E_h, in hartree) for the *S*, *T* and *C* conformations of compounds **1**–**3**.

Geometry	Method						
	MP2/6-311+G**//MP2/6-311+G**				B3LYP/6-311+G**//MP2/6-311+G**		
	ZPE	$E_{el.}$	E_0	ΔE_0[a]	$E_{el.}$	E_0	ΔE_0[a]
1-*S*	0.026808	−151.242552	−151.215744	0.000000 (0.00)[b]	−151.601991	−151.575183	0.000000 (0.00)[b]
1-*T*	0.025996	−151.240972	−151.214976	0.000768 (0.48)[b] (0.86)[c] (1.11)[d]	−151.600764	−151.574768	0.000415 (0.26)[b]
1-*C*	0.025820	−151.228291	−151.202471	0.013273 (8.33)[b] (3.72)[c] (7.33)[d]	−151.588487	−151.562667	0.012516 (7.85)[b]
2-*S*	0.019000	−796.499033	−796.480033	0.000000 (0.00)[b]	−797.633903	−797.614903	0.000000 (0.00)[b]
2-*T*	0.018025	−796.490592	−796.472567	0.007466 (4.68)[b] (6.00)[e]	−797.626026	−797.608001	0.0069029 (4.33)[b]
2-*C*	0.017898	−796.486487	−796.468589	0.011444 (7.18)[b] (9.30)[e]	−797.622056	−797.604158	0.010745 (6.74)[b]
3-*S*	0.016328	−4801.027251	−4801.010923	0.000000 (0.00)[b]	−4804.318360	−4804.302032	0.000000 (0.00)[b]
3-*T*	0.015466	−4801.019266	−4801.003800	0.007123 (4.47)[b]	−4804.310642	−4804.295176	0.0068562 (4.30)[b]
3-*C*	0.015411	−4801.016433	−4801.001022	0.009901 (6.21)[b]	−4804.308097	−4804.292686	0.009346 (5.86)[b]

[a] Relative to the ground state.
[b] Numbers in parenthesis are the corresponding thermodynamic functions values in kcal mol^{-1}.
[c] Experimental from IR, see Ref. [28].
[d] Experimental from IR, see Ref. [29].
[e] Experimental from MW, see Refs. [31–33].

3. Results and discussion

3.1. Conformational interconversions

The zero point (*ZPE*) and total electronic (E_{el}) energies ($E_o = E_{el} + ZPE$) for the ground state [skew (*S*)] and transition state [trans (*T*) and cis (*C*)] conformations of compounds **1**–**3**, as calculated at the MP2/6-311+G** level of theory, are given in Table 1. For single-point energy calculations, the hybrid-density functional theory (hybrid-DFT: B3LYP/6-311+G**//MP2/6-311+G**) based method was used. Results of the two approaches are in agreement with each other and with available experimental data within the somewhat large variability of the latter (see Table 1). Table 2 shows the value of the thermodynamic functions H, S, G and the ΔG, ΔS and ΔH parameters, as calculated at the MP2/6-311+G** level of theory. Since the ΔS values are relatively small, the calculated ΔH and ΔG parameters are close to the ΔE_0 values.

Table 2
MP2/6-311+G**//MP2/6-311+G** calculated thermodynamic functions [enthalpies, Gibbs free energies at 298.15 K and 1 atm (in kcal mol^{-1}) and entropies (in cal mol^{-1} K^{-1}) in the standard condition (T = 298 K and P = 1 atm)] for the *S*, *T* and *C* conformations of compounds **1**–**3**.

Geometries	*H*	*S*	*G*	ΔH[a]	ΔS[a]	ΔG[a]
1-*S*	−94886.78	54.28	−94902.96	0.00	0.00	0.00
1-*T*	−94886.50	54.69	−94902.80	0.28	0.41	0.16
1-*C*	−94878.65	54.70	−94894.96	8.13	0.42	8.00
2-*S*	−499796.44	60.24	−499814.40	0.00	0.00	0.00
2-*T*	−499791.91	60.91	−499810.07	4.53	0.67	4.33
2-*C*	−499789.41	60.95	−499807.59	7.03	0.71	6.81
3-*S*	−3012679.40	66.57	−3012699.25	0.00	0.00	0.00
3-*T*	−3012675.12	67.07	−3012695.12	4.28	0.50	4.13
3-*C*	−3012673.38	67.10	−3012693.38	6.02	0.53	5.87

[a] Relative to the ground state (*S* conformation).

Tables 3 and 4 show the results of similar calculations using CBS methods. The CBS-QB3 and CBS-4 energies agree with those from our methods within the errors established for those methods on the G2 test set [54] and give comparable agreement with the available experimental measurements. There seems no reason for choosing between either of these or the two methods we used originally. However, the CBS-Q method has serious problems. First it erroneously selects the C conformers of compounds **1** and **2** and the *T* conformation of compound **3** as the minimum energy forms in disagreement with all the other computational and experimental evidence. Further, and probably not unrelated to this, all energy differences are calculated to be nearly an order of magnitude smaller than from any of the other methods. These conclusions are, of course, also reflected by comparison of the thermodynamic values in Tables 2 and 4. Further work described here makes use of our original methods.

There are two distinct transition states (excluding the mirror image pathways), which are required to describe the dynamic conformational properties of compounds **1**–**3** (see Fig. 1). Since the *T* and *C* conformations of compounds **1**–**3** are true transition states, the racemization processes of the axial symmetrical *S* conformations of compounds **1**–**3** could take place by passing through their *T* or *C* conformations are shown in Table 1. The calculated energy barriers for the interconversion processes in compounds **1**–**3** between the *S* conformations and their mirror image conformations *via* *T* transition state structures ($S \rightarrow [T]^{\ddagger} \rightarrow S'$) are 0.48, 4.68 and 4.47 kcal mol^{-1}, respectively, as calculated by the MP2/6-311+G**//MP2/6-311+G** level or 0.26, 4.33 and 4.30 kcal mol^{-1}, respectively, using the B3LYP/6-311+G**//MP2/6-311+G** level. In addition, the racemization process of the *S* conformations can take place *via* other pathways (i.e. by passing through the *C* transition state structures). The results are calculated barrier heights for the interconversion processes of *S* and its mirror image in compounds

Table 3
CBS-QB3, CBS-Q and CBS-4 calculated zero-point energies *ZPE*, thermal-corrected energies ($E = E_o + E_{trans} + E_{rot} + E_{vib}$), and relative energies ΔE (E_h, in hartree) for the *S*, *T* and *C* conformations of compounds **1**–**3**.

Geometry	CBS-QB3			CBS-Q			CBS-4		
	ZPE	*E*	ΔE[a]	*ZPE*	*E*	ΔE[a]	*ZPE*	*E*	ΔE[a]
1-*S*	0.026198	−151.375349	0.000000 (0.00)[b]	0.026965	−151.372916	0.001168 (0.73)[b]	0.024748	−151.384852	0.000000 (0.00)[b]
1-*T*	0.025601	−151.374610	0.000739 (0.46)[b] (0.86)[c] (1.11)[d]	0.026243	−151.373992	0.000092 (0.06)[b]	0.024727	−151.384735	0.000117 (0.07)[b]
1-*C*	0.025356	−151.364477	0.010872 (6.82)[b] (3.72)[c] (7.33)[d]	0.026158	−151.374084	0.000000 (0.00)[b]	0.024354	−151.374336	0.010516 (6.60)[b]
2-*S*	0.018027	−796.678300	0.000000 (0.00)[b]	0.018565	−796.676534	0.001319 (0.83)[b]	0.018453	−796.670450	0.000000 (0.00)[b]
2-*T*	0.017123	−796.670551	0.007749 (4.86)[b] (6.00)[e]	0.017563	−796.677785	0.000068 (0.04)[b]	0.017430	−796.662195	0.008255 (5.18)[b]
2-*C*	0.016974	−796.667149	0.011151 (7.00)[b] (9.30)[e]	0.017500	−796.677853	0.000000 (0.00)[b]	0.017363	−796.658294	0.012156 (7.63)[b]
3-*S*	0.015366	−4801.713626	0.000000 (0.00)[b]	0.015733	−4801.706761	0.001121 (0.70)[b]	0.015849	−4801.343272	0.000000 (0.00)[b]
3-*T*	0.014602	−4801.706843	0.006783 (4.26)[b]	0.014910	−4801.707882	0.000000 (0.00)[b]	0.015021	−4801.336201	0.007071 (4.44)[b]
3-*C*	0.014503	−4801.704105	0.009521 (5.97)[b]	0.014926	−4801.707847	0.000035 (0.02)[b]	0.015037	−4801.333378	0.009894 (6.21)[b]

[a] Relative to the ground state.
[b] Numbers in parenthesis are the corresponding thermodynamic functions values in kcal mol^{-1}.
[c] Experimental from IR, see Ref. [28].
[d] Experimental from IR, see Ref. [29].
[e] Experimental from MW, see Refs. [31–33].

1–**3** *via C* transition state structures ($S \rightarrow [C]^{\ddagger} \rightarrow S'$) are 8.33, 7.18 and 6.21 kcal mol^{-1}, or 7.85, 6.74 and 5.86 kcal mol^{-1}, by the two methods.

In addition, MP2/6-311+G**//MP2/6-31G+G** results showed that the calculated Gibbs free energy difference (G_T–G_S) values (ΔG_{T-S}) between the *S* and *T* conformations of compounds **1**–**3** are 0.16, 4.33 and 4.13 kcal mol^{-1}, respectively, while the calculated ΔG_{C-S} between the skew *S* and *C* conformations of compounds **1**–**3** are 8.00, 6.81 and 5.87 kcal mol^{-1} (see Table 2). Thus in compounds **1** and **2**, the conformational interconversion processes between the *S* conformations and their mirror image forms (*S*′) should take place *via* the *T* transition state structure. For compound **3**, there are two possible pathways with nearly equal energies (see Fig. 1). Importantly, the calculated barrier heights for $S \rightarrow [T]^{\ddagger} \rightarrow S'$ and $S \rightarrow [C]^{\ddagger} \rightarrow S'$ interconversion processes for compounds **1** and **2** are in good agreement with reported experimental and theoretical results [27–29,34,35,40].

3.2. Stabilization energies

According to the NBO results, the *S* conformations of compounds **1**–**3** benefit from the resonance energies associated with $LP_2M2 \rightarrow \sigma^*_{M3\text{-}H4}$ electronic delocalizations. Based on the optimized ground state geometries at the MP2/6-311+G** level of theory, the NBO analysis of donor–acceptor (bond-antibond) interactions showed that the stabilization energies associated with $LP_2M2 \rightarrow \sigma^*_{M3\text{-}H4}$ delocalizations for the *S* conformations of compounds **1**–**3** are 1.35, 5.94 and 4.68 kcal mol^{-1}, respectively (see Table 5). Interestingly, the variations of the stabilization energies associated with $LP_2M2 \rightarrow \sigma^*_{M3\text{-}H4}$ electronic delocalizations is in accordance with the variations of the $S \rightarrow [T]^{\ddagger} \rightarrow S'$ barrier heights from compound **1** to compound **3**.

3.3. Orbital occupancies

NBO results showed that the LP_2M2 nonbonding orbital occupancies of the *S* conformations decrease from compound **1** to

Table 4
CBS-QB3, CBS-Q and CBS-4 calculated thermodynamic functions [-enthalpies, Gibbs free energies at 298.15 K and 1 atm (in kcal mol^{-1}) and entropies (in cal mol^{-1} K^{-1}) in the standard condition (T = 298 K and P = 1 atm)] for the *S*, *T* and *C* conformations of compounds **1**–**3**.

Geometry	CBS-QB3			CBS-Q			CBS-4		
	ΔH[a]	ΔS[a]	ΔG[a]	ΔH[a]	ΔS[a]	ΔG[a]	ΔH[a]	ΔS[a]	ΔG[a]
1-*S*	0.000	0.000	0.000	0.73	1.372	0.32	0.000	0.000	0.000
1-*T*	0.46	−1.187	0.82	0.06	0.000	0.000	0.07	−1.084	0.40
1-*C*	6.82	−1.174	7.17	0.000	−1.189	0.35	6.60	−5.219	8.16
2-*S*	0.000	0.000	0.000	0.83	0.686	0.58	0.000	0.000	0.000
2-*T*	4.86	−2.033	5.47	0.06	0.042	0.05	5.18	−0.654	5.38
2-*C*	7.00	−0.600	7.18	0.000	0.000	0.000	7.63	0.745	7.41
3-*S*	0.000	0.000	0.000	0.70	0.940	0.42	0.000	0.000	0.000
3-*T*	4.26	−0.890	4.52	0.000	0.000	0.000	4.44	0.440	4.31
3-*C*	5.97	−0.867	6.22	0.02	0.000	0.02	6.21	0.444	6.08

[a] Relative to the ground state (*S* conformation).

Table 5
Calculated second order perturbational (resonance) energies (E_2), F_{ij} (off-diagonal elements), orbital energies, orbital energy differences, orbital occupancies and M atom hybridized orbitals in the most stable [i.e. skew (*S*)] conformations of compounds **1**–**3** using NBO analysis, based on the structures optimized at the MP2/6-311+G** level of theory.

	Compound		
	1-*S*	**2**-*S*	**3**-*S*
E_2 (resonance energy, kcal mol^{-1})			
$LP_2M2 \rightarrow \sigma^*_{M3\text{-}H4}$	1.35	5.94	4.68
F_{ij} (off-diagonal element)			
$LP_2M2 \rightarrow \sigma^*_{M3\text{-}H4}$	0.036	0.060	0.050
Orbital energy			
E_{LP_2M2}	−0.54734	−0.40509	−0.37530
$E\sigma^*_{M3\text{-}H4}$	0.67669	0.36153	0.29916
$\Delta(E\sigma^*_{M3\text{-}H4} - E_{LPM2})$	1.22	0.77	0.67
Orbital occupancy			
E_{LP_2M2}	1.99531	1.98032	1.98293
$E\sigma^*_{M3\text{-}H4}$	0.00300	0.01751	0.01573
μ (Debye)	1.8192	1.5383	1.0758
M atom hybridized orbital			
M–H	$sp^{3.40}d^{0.01}$	$sp^{5.74}d^{0.06}$	$sp^{6.60}d^{0.06}$
M–M	$sp^{7.07}d^{0.02}$	$sp^{7.54}d^{0.09}$	$sp^{10.03}d^{0.12}$
Bond order (Wiberg Bond Index)			
M–M	1.0081	1.0377	1.0358

compound **3**, but increase from compound **2** to compound **3**, and inversely, the $\sigma^*_{M3\text{-}H4}$ nonbonding orbital occupancies of the *S* conformations increase from compound **1** to compound **2** but decrease from compound **2** compound **3** (see Table 5). Since the $LP_2M2 \rightarrow \sigma^*_{M3\text{-}H4}$ electronic delocalizations give rise to charge transfer from LP_2M2 to $\sigma^*_{M3\text{-}H4}$, this fact can justify the charge depletion of the donor orbital and also the charge accumulation of the acceptor orbital.

3.4. Orbital energies and off-diagonal elements

It should be noted that the stabilization energy associated with the interaction between an occupied LP orbital and an unoccupied σ^* orbital is proportional to $S^2/\Delta E$ where *S* is the overlap integral and ΔE is their energy separation. As *S* increases and also ΔE decreases, the $LP \rightarrow \sigma^*$ conjugative interaction become stronger. Therefore, these two factors can play a key role on the conformational properties of compounds **1**–**3**. The energy difference between donor (E_{LP_2M2}) and acceptor ($E\sigma^*_{M3\text{-}H4}$) orbitals for the *S* conformations of compounds **1**–**3** are 1.22, 0.77 and 0.67 a.u., respectively, as calculated by NBO analysis. Effectively, the energy differences between donor (E_{LP_2M2}) and acceptor ($E\sigma^*_{M3\text{-}H4}$) orbitals increase from the *S* conformations of compound **1** to compound **3**. It can be concluded that the strong acceptor antibonding orbital of compound **3**, compared to those in compounds **2** and **1** may gives rise to strong resonance energy, but the decrease of the *orbital overlap* (*S*) [off-diagonal elements (F_{ij})] values could reduce the resonance energy (see Table 5). NBO calculated off-diagonal elements (F_{ij}) for $LP_2M2 \rightarrow \sigma^*_{M3\text{-}H4}$ electronic delocalizations in the *S* conformations of compounds **1**–**3** are 0.036, 0.060 and 0.050, respectively. This fact can explain the increase of the resonance energy associated with $LP_2M2 \rightarrow \sigma^*_{M3\text{-}H4}$ electronic delocalizations from the *S* conformations of compound **1** to compound **2** and also the decrease of the resonance energy from compound **2** to compound **3**.

3.5. Dipole moments

It is well known that there is a preference for the conformation with the smallest dipole moment. Especially in the gas phase it is generally found that the conformation with the larger dipole moment has the larger electrostatic energy and therefore an increased overall energy [58]. Calculated dipole moments for the *S* conformations of compounds **1**–**3** are given in Table 5. The MP2/6-311+G** results showed that the calculated dipole moment values decrease from the *S* conformations of compound **1** to compound **3**. Based on these results, the rationalization of the conformational properties solely in terms of dipole moments succeeds in accounting qualitatively for the greater conformational mobility of the *S* conformation of compound **1**, compared to compound **2**, but fails to account for the decrease of the conformational mobility from compound **2** to compound **3** (see Table 5).

3.6. Bond orders

The $LP_2M2 \rightarrow \sigma^*_{M3\text{-}H4}$ electronic delocalizations can affect the bond orders of M–M bonds of compounds **1**–**3** (see Scheme 2). Based on the results obtained, the calculated bond orders [Wiberg Bond Index (WBI)] for M–M bonds of the *S* conformations of compounds **1**–**3** are 1.0081, 1.0377 and 1.358, respectively. The variation of the calculated WBI values for M–M bonds of the *S* conformations of compounds **1**–**3** is in accordance with the variation of the $LP_2M2 \rightarrow \sigma^*_{M3\text{-}H4}$ electronic delocalizations and also the calculated energy barriers for $S \rightarrow [T]^{\ddagger} \rightarrow S'$ interconversion processes from compound **1** to compound **3** (see Table 5).

3.7. Structural parameters

Representative structural parameters for the *S*, *T* and *C* conformations of compounds **1**–**3** as calculated at the MP2/6-311+G** level of theory are shown in Table 6. Due to the various definitions of bond lengths, it is not expected, in principal, to obtain the experimental values exactly, however, it is possible to carry out theoretical calculations with an accuracy that is enlightening in our discussion of conformational preference. Importantly, consideration of the precise structures of the *S*, *T* and *C* conformations of compounds **1**–**3** (optimized at the MP2/6-311+G** level of theory), gives evidence that in the *S* conformations of compounds **1**–**3**, the σ_{M-M} bond lengths are significantly contracted, compared to those in the *T* and *C* conformations. On the other hand, the σ_{M-H} bond lengths in the *S* conformations of compounds **1**–**3** are longer than those in their *T* conformations. Interestingly, the longer σ_{M-H} bonds and also the shorter σ_{M-M} bond lengths in the ground state (i.e. *S* conformations) structures of compounds **1**–**3**, could be the result of $LP_2M2 \rightarrow \sigma^*_{M3\text{-}H4}$ electronic delocalizations (see Scheme 2).

In addition, the calculations results showed that the $\theta_{\mathbf{1\text{-}2\text{-}3}}$ bond angles of the *S* conformations decrease from compound **1** to compound **3**. Also, the $\phi_{H\text{-}M\text{-}M\text{-}H}$ in the *S* conformations decreased from compound **1** to compound **3** (see Table 4). The decrease of the $\theta_{1\text{-}2\text{-}3}$ bond angles and the $\phi_{H\text{-}M\text{-}M\text{-}H}$ dihedral angles in the *S* conformations from compound **1** to compound **3** can be explained by the increase of the *p* and *d* orbital participation in the M atom hybiridized orbitals in the M–M and N–H bonds (see Table 5). In this regard, NBO analysis revealed that the M atom hybridized orbitals

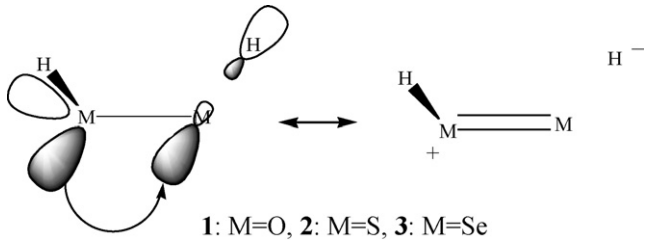

1: M=O, **2**: M=S, **3**: M=Se

Scheme 2.

Table 6
MP2/6-311+G** calculated structural parameters of the *S*, *T* and *C* conformations of compounds **1**–**3**.

State	Compound								
	1			**2**			**3**		
	S	*T*	*C*	*S*	*T*	*C*	*S*	*T*	*C*
Bond lengths (Å)									
r_{M-H}	0.965 (0.967)[f] (0.950)[g] (0.967)[h] (0.965)[e]	0.964	0.965	1.337 (1.342)[a] (1.327)[b] (1.336)[c] (1.355)[d] (1.337)[e]	1.334	1.334	1.463 (1.507)[i]	1.461	1.560
r_{M-M}	1.450 (1.463)[f] (1.475)[g] (1.456)[h] (1.450)[e]	1.459	1.458	2.083 (2.056)[a] (2.055)[b] (2.082)[c] (2.112)[d] (2.083)[e]	2.125	2.137	2.356 (2.376)[i]	2.398	2.409
Bond angles (°)									
θ_{H-M-M}	99.6 (99.3)[f] (94.8)[g] (102.3)[h] (99.6)[c]	98.3	104.3	98.1 (97.9)[a] (91.3)[b] (98.1)[c] (98.4)[d] (98.1)[e]	92.8	96.3	96.1 (95.5)[i]	91.0	94.0
Torsion angles (°)									
$\phi_{1-2-3-4}$	121.3 (121.5)[e] (111.9)[f]	180.0	0.0	90.82 (90.3)[a] (90.4)[c] (88.7)[h] (90.3)[d] (90.9)[e]	180.0	0.0	90.5	180.0	0.0

[a] From IR and MW, see Ref. [41].
[b] From MW, see Ref. [32].
[c] From MP2/6-311G**, see Ref. [20].
[d] From CASSCF/ANO-S, see Ref. [20].
[e] From MP2(FC)/6-311++G**, see Ref. [30].
[f] From IR, see Ref. [29].
[g] From IR, see Ref. [28].
[h] By fitting the calculated rotational constants to the observed values, see Ref. [36].
[i] From HF/STO-4G, see Ref. [26].

for the M–M bonds in the ground state structures (*S* conformations) of compounds **1**–**3** are sp $^{7.07}$d$^{0.02}$, sp $^{7.54}$d$^{0.09}$ and sp $^{10.03}$d$^{0.12}$, respectively. Also, the M atom hybridized orbitals for the M–H bonds in the *S* conformations of compounds **1**–**3** are sp $^{3.40}$d$^{0.01}$, sp $^{5.74}$d$^{0.06}$ and sp $^{6.60}$d$^{0.06}$, respectively.

4. Conclusions

The above reported ab initio, hybrid-DFT and NBO analysis provide a reasonable picture from structural, energetic, bonding and stereoelectronic points of view for the conformational properties of compounds **1**–**3**. Effectively, the results showed that the racemization processes of the axial symmetrical *S* conformations of compounds **1**–**3** can take place by passing through the *T* transition state conformations, while the barriers of $S \rightarrow [C]^{\ddagger} \rightarrow S'$ interconversions are higher.

In addition, the NBO results revealed that:

- the stabilization energies associated with $LP_2M2 \rightarrow \sigma^*_{M3\text{-}H4}$ electronic delocalizations increase from the *S* conformations of compound **1** to compound **2**, but decrease from compound **2** to compound **3**. The variations of the stabilization energies associated with $LP_2M2 \rightarrow \sigma^*_{M3\text{-}H4}$ electronic delocalizations is in accordance with the variations of the $S \rightarrow [T]^{\ddagger} \rightarrow S'$ barrier heights from compound **1** to compound **3**.
- the variations of the stabilization energies associated with $LP_2M2 \rightarrow \sigma^*_{M3\text{-}H4}$ electronic delocalizations could reasonably explain the variations of the LP_2M2 nonbonding and the $\sigma^*_{M3\text{-}H4}$ antibonding orbital occupancies in the most stable (*S*) conformations of compounds **1**–**3**.
- the energy difference between donor (E_{LP_2M2}) and acceptor ($E\sigma^*_{M3\text{-}H4}$) orbitals [i.e. $\Delta(E\sigma*_{M3\text{-}H4} - E_{LP_2M2})$] increased from the *S* conformations of compound **1** to compound **3**. It can be concluded that the stronger acceptor antibonding orbital of compound **3**, compared to those in compounds **2** and **1**, may give rise to strong resonance energy, but the decrease of the *orbital overlap* (*S*) [off-diagonal elements (F_{ij})] values could reduce the resonance energy.
- the rationalization of the conformational properties solely in terms of dipole moments succeeded in accounting qualitatively for the increase of conformational mobility of the *S* conformation of compound **1**, compared to compound **2**, but fails to account the increase of the conformational mobility from compound **2** to compound **3**.

The longer σ_{M-H} bonds and also the shorter σ_{M-M} bond lengths in the *S* conformations of compounds **1**–**3**, can be the result of the $LP_2M2 \rightarrow \sigma^*_{M3\text{-}H4}$ electronic delocalization. The decrease of the $\theta_{1\text{-}2\text{-}3}$ bond angles and the $\phi_{H-M-M-H}$ dihedral angles in the *S* conformations of compounds **1**–**3** is explained by the increase of the *p* and *d* orbital percentages of the M atom hybiridized orbitals in the M–M and M–H bonds from the *S* conformations of **1** to compound **3**.

Acknowledgement

The part of this work done at the University of Texas at Austin has been supported by Grant No. F-100 from the Welch Foundation.

References

[1] J.H. Steinfeld, S.N. Pandis, Atmospheric Chemistry and Physics, J. Wiley Interscience, New York, 1998.
[2] M.R. Hofmann, J.O. Edwards, Kinetics of the oxidation of sulfite by hydrogen peroxide in acidic solution, J. Phys. Chem. 79 (1975) 2096–2098.
[3] S.A. Penkett, B.M.R. Jones, K.A. Brice, A.E.J. Eggleton, The importance of atomospheric ozone and hydrogen peroxide in oxidizing sulfur dioxide in cloud and rainwater, Atmos. Environ. 13 (1979) 123–137.
[4] L.M. Martin, D.E. Damschen, Aqueous oxidation of sulfur dioxide by hydrogen peroxide at low Ph, Atmos. Environ. 15 (1981) 1615–1622.
[5] S.M. Kunen, A.L. Lazrus, G.L. Kok, B.G. Heikes, Aqueous oxidation of SO_2 by hydrogen peroxide, J. Geophys. Res. 88 (1983) 3671–3674.
[6] J.V. McArdle, M.R. Hoffmann, Kinetics and mechanism of the oxidation of aquated sulfur dioxide by hydrogen peroxide at low pH, J. Phys. Chem. 87 (1983) 5425–5429.
[7] L.I. Klienman, Seasonal dependence of boundary layer peroxide concentrations: the low and high NOx regimes, J. Geophys. Res. 96 (1991) 20721–20733.
[8] M.C. Daza, J.A. Dobada, J.M. Molina, P. Salvador, M. Duran, J.L. Villaveces, Basis set superposition error-counterpoise corrected potential energy surfaces. Application to hydrogen peroxide. . .X (X = F^-, Cl^-, Br^-, Li^+, Na^+) complexes, J. Chem. Phys. 110 (1999) 11806–11813, and references therein.
[9] B.-M. Cheng, W.-C. Hung, Photoionization efficiency spectrum and ionization energy of HSSH produced from gaseous self-reaction of HS radicals, J. Phys. Chem. 100 (1996) 10210–10214.
[10] F. Franzfehër, H. Münzner, Ultraviolett-Absorptionsspektren kettenförmiger Schwefelverbindungen, Chem. Ber. 96 (1963) 1131–1147.
[11] R.K. Gosavi, M. DeSorgo, H.E. Gunning, O.P. Strausz, The UV absorption spectrum and geometry of the HS2 radical, Chem. Phys. Lett. 21 (1973) 318–321.
[12] S.W. Benson, Thermochemistry and kinetics of sulfur-containing molecules and radicals, Chem. Rev. 78 (1978) 23–35.
[13] K.J. Holstein, E.H. Fink, J. Wildt, F. Zabel, Ã2A' » $\tilde{X}$ 2A« emission spectrum of the HS2 radical, Chem. Phys. Lett. 113 (1985) 1–7.
[14] C.J. Marsden, B.J. Smith, Harmonic force field, molecular structure, torsional potential, and possible isomerism of hydrogen sulfide (H_2S_2), J. Phys. Chem. 92 (1988) 347–353.
[15] T.-K. Ha, W. Cencek, Ab initio CI study of the optical rotatory strengths of HSSH, Chem. Phys. Lett. 182 (1991) 519–523.
[16] P. Mittler, K.M.T. Yamada, G. Winnewisser, M. Birk, High-resolution FTIR spectrum of HSSH in the SH-stretching region: the ν5 band, J. Mol. Spectrosc. 164 (1994) 390–394.
[17] D.R. Alleres, D.L. Cooper, T.P. Cunningham, J. Garrett, P.B. Karadakov, M. Ramimondi, Bonding in YXXY dihalides and dihydrides of dioxygen and disulfur, J. Chem. Faraday Trans. 91 (1995) 3357–3362.
[18] K.M.T. Yamada, J. Behrend, S.P. Belov, G. Winnewisser, Anomalous K-type doubling of HSSH, J. Mol. Spectrosc. 176 (1996) 397–402.
[19] J. Koput, An ab initio study on the equilibrium structure and torsional potential energy function of disulfane, Chem. Phys. Lett. 259 (1996) 146–150.
[20] R. Steudel, Y. Drozdova, K. Miaskiewicz, R.H. Hertwig, W. Koch, How unstable are thiosulfoxides? An ab initio MO study of various disulfanes RSSR (R = H, Me, Pr, All), their branched isomers R2SS, and the related transition states, J. Am. Chem. Soc. 119 (1997) 1990–1996.
[21] B.S. Jursic, Computation of bond dissociation energy for sulfides and disulfides with ab initio and density functional theory methods, Int. J. Quantom Chem. 62 (1997) 291–302.
[22] M. Pericou-Cayere, M. Galize, A. Dargelos, Ab initio calculations of electronic spectra of H_2S and H_2S_2, Chem. Phys. 214 (1997) 81–89.
[23] R. Benassi, F. Taddei, A theoretical ab initio approach to the S–S bond breaking process in hydrogen disulfide and in its radical anion, J. Phys. Chem. 102 (1998) 6173–6180.
[24] O.M. Suleimenev, T.-K. Ha, Ab initio calculation of the thermochemical properties of polysulphanes (H_2S_n), Chem. Phys. Lett. 290 (1998) 451–457.
[25] D.W. Matula, L.C.D. Groenweghe, J.R. Van Wazer, Molecular distributions at equilibrium. I. Theory of equilibria in scrambling reactions and interpretation of NMR spectra, J. Chem. Phys. 41 (1964), 3105-3022.
[26] C.S. Ewig, E.H. Mei, J.R. Van Wazar, Rotational barriers in H_2Se_2 and H_2Te_2, Mol. Phys. 40 (1980) 241–245.
[27] M.S. Gordon, Molecular orbital study of internal rotation, J. Am. Chem. Soc. 91 (1969) 3122–3130.
[28] R.L. Readington, W.B. Olson, P.S. Cross, Studies of hydrogen peroxides: the infrared spectrum and the internal rotation problem, J. Chem. Phys. 36 (1962) 1311–1326.
[29] J. Flaud, C. Camy-Peyret, J.W.C. Johns, B. Carli, The far infrared spectrum of H_2O_2. First observation of the staggering of the levels and determination of the cis barrier, J. Chem. Phys. 91 (1989) 1504–1510.
[30] S. Samdal, V.S. Mastryukov, J.E. Boggs, Structural changes as a function of torsional motion studied by ab initio calculations Part 4. The dependence of the dynamic behavior of the structural parameters for H_2O_2 and H_2S_2 on basis sets and comparison with experimental results, J. Mol. Struct. 346 (1995) 35–40.
[31] A. Veillard, J. Dmuynk, Barrier to internal rotation in hydrogen persulphide, Chem. Phys. Lett. 4 (1970) 476–478.
[32] G. Winnewisser, M. Winnewisser, W. Gordy, Millimeter-wave rotational spectrum of HSSH and DSSD* I. Q branches, J. Chem. Phys. 49 (1968) 3465–3478.
[33] M.E. Schwartz, Theoretical study of the barriers to internal rotation in hydrogen persulfide, H_2S_2, J. Chem. Phys. 51 (1969) 4182–4286.
[34] D.A. Dixon, D. Zeroka, J.J. Wendoloski, Z.R. Wasserman, The molecular structure of H,S, and barriers to internal rotation, J. Phys. Chem. 89 (1985) 5334–5336.
[35] J. Behrend, P. Mittler, G. Winnewisser, K.M.T. Yamada, Spectra of deuterated disulfane and spectroscopic determination of its molecular structure, J. Mol. Spectrosc. 150 (1991) 99–119.
[36] G. Pelz, K.M.T. Yamada, G. Winnewisser, Torsional dependence of the effective rotational constants of H_2O_2 and H_2S_2, J. Mol. Spectrosc. 159 (1993) 507–520.
[37] A. Rauk, Chiroptical properties of disulfides. Ab initio studies of dihydrogen disulfide and dimethyl disulfide, J. Am. Chem. Soc. 106 (1984) 6517–6524.
[38] A. Rastelli, M. Cocchi, Model calculations of chemical interactions. Part 3. Rotational energy profiles in simple molecules: evaluation, additivity and role of bond–bond, bond–lone–pair and lone–pair–lone–pair interactions, J. Chem. Soc., Faraday Trans. 87 (1991) 249–258.
[39] I. Cárdenas-Jirón, C. Cárdenas-Laihacar, A. Toro-Labbe, On the rotational isomerism of one rotor molecules. A comparative study of the HSSH and HXNX (X = O, S) series of molecules, J. Mol. Struct. (Theochem.) 210 (1990) 279–290.
[40] A. Hinchcliffe, Structure and properties of HSSH, H_2SS, FSSF and F_2SS, J. Mol. Struct. 55 (1979) 127–134.
[41] J. Hahn, P. Schmidt, K. Reinartz, J. Behrend, G. Winnewisser, K.M.T. Yamada, Synthesis and molecular structure of disulfane, Z. Naturforsch. B 46 (1991) 1338–1342.
[42] M.J. Frisch, G.W. Trucks, H.B. Schlegel, G.E. Scuseria, M.A. Robb, J.R. Cheeseman, J.A. Montgomery Jr., T. Vreven, K.N. Kudin, J.C. Burant, J.M. Millam, S.S. Iyengar, J. Tomasi, V. Barone, B. Mennucci, M. Cossi, G. Scalmani, N. Rega, G.A. Petersson, H. Nakatsuji, M. Hada, M. Ehara, K. Toyota, R. Fukuda, J. Hasegawa, M. Ishida, T. Nakajima, Y. Honda, O. Kitao, H. Nakai, M. Klene, X. Li, J.E. Knox, H.P. Hratchian, J.B. Cross, V. Bakken, C. Adamo, J. Jaramillo, R. Gomperts, R.E. Stratmann, O. Yazyev, A.J. Austin, R. Cammi, C. Pomelli, J.W. Ochterski, P.Y. Ayala, K. Morokuma, G.A. Voth, P. Salvador, J.J. Dannenberg, V.G. Zakrzewski, S. Dapprich, A.D. Daniels, M.C. Strain, O. Farkas, D.K. Malick, A.D. Rabuck, K. Raghavachari, J.B. Foresman, J.V. Ortiz, Q. Cui, A.G. Baboul, S. Clifford, J. Cioslowski, B.B. Stefanov, G. Liu, A. Liashenko, P. Piskorz, I. Komaromi, R.L. Martin, D.J. Fox, T. Keith, M.A. Al-Laham, C.Y. Peng, A. Nanayakkara, M. Challacombe, P.M.W. Gill, B. Johnson, W. Chen, M.W. Wong, C. Gonzalez, J.A. Pople, Gaussian 03, Revision B.03, Gaussian Inc., Wallingford, CT, 2004.
[43] A.D. Becke, Density-functional thermochemistry. III. The role of exact exchange, J. Chem. Phys. 98 (1993) 5648–5652.
[44] C. Lee, W. Yang, R.G. Parr, Development of the Colle-Salvetti correlation-energy formula into a functional of the electron density, Phys. Rev. B 37 (1988) 785–789.
[45] W.J. Hehre, L. Radom, P.V.R. Schleyer, J.A. Pople, Ab initio Molecular Orbital Theory, Wiley, New York, 1986.
[46] J.M. Seminario, P. Politzer (Eds.), Modern Density Function Theory, A Tool for Chemistry, Elsevier, Amsterdam, 1995.
[47] N.B. Epiotis, R.L. Yates, R.J. Larson, C.R. Kirmaier, F. Bernardi, Directional effects of σ conjugation on geometrical isomerism, J. Am. Chem. Soc. 99 (1977) 8379–8388.
[48] E.D. Glendening, A.E. Reed, J.E. Carpenter, F. Weinhold, 2001, NBO Version 3.1. Theoretical Chemistry Institute, University of Wisconsin, Madison, Wisconsin, USA.
[49] A.E. Reed, L.A. Curtiss, F. Weinhold, Intermolecular interactions from a natural bond orbital, donor–acceptor viewpoint, Chem. Rev. 88 (1988) 899–926.
[50] P. Dionne, M. St-Jacques, Mechanism of the gauche conformational effect in 3-halogenated 1,5-benzodioxepins, J. Am. Chem. Soc. 109 (1987) 2616–2623.
[51] M.R. Nyden, G.A. Petersson, Complete basis set correlation energies. I. The asymptotic convergence of pair natural orbital expansions, J. Chem. Phys. 75 (1981) 1843–1862.
[52] G.A. Petersson, M.A. Al-Laham, A complete basis set model chemistry. II. Open-shell systems and the total energies of the first-row atoms, J. Chem. Phys. 94 (1991) 6081–6090.
[53] G.A. Petersson, T.G. Tensfeldt, J.A. Montgomery Jr., A complete basis set model chemistry. III. The complete basis set-quadratic configuration interaction family of methods, J. Chem. Phys. 94 (1991) 6091–6101.
[54] J.W. Ochterski, G.A. Petersson, J.A. Montgomery Jr., A complete basis set model chemistry. V. Extensions to six or more heavy atoms, J. Chem. Phys. 104 (1996) 2598–2619.
[55] G.A. Petersson, D.K. Malick, W.G. Wilson, J.W. Ochterski, J.A. Montgomery Jr., M.J. Frisch, Calibration and comparison of the Gaussian-2, complete basis set, and density functional methods for computational thermochemistry, J. Chem. Phys. 109 (1998) 10570–10579.
[56] J.A. Montgomery Jr., M.J. Frisch, J.W. Ochterski, G.A. Petersson, A complete basis set model chemistry. VI. Use of density functional geometries and frequencies, J. Chem. Phys. 110 (1999) 2822–2827.
[57] J.A. Montgomery Jr., M.J. Frisch, J.W. Ochterski, G.A. Petersson, A complete basis set model chemistry. VII. Use of the minimum population localization method, J. Chem. Phys. 112 (2000) 6532–6542.
[58] K.B. Wiberg, M.A. Murcko, Rotational barriers. 1. 1,2-Dihaloethanes, J. Phys. Chem. 91 (1987) 3616–3620.